Current Research in Green and Sustainable Chemistry 4 (2021) 100103

Contents lists available at ScienceDirect

Current Research in Green and Sustainable Chemistry

journal homepage: www.elsevier.com/journals/current-research-in-green-and-sustainable-chemistry/2666-0865

Sustainable fabrication, optical properties and rapid performance of bio-engineered copper nanoparticles in removal of toxic methylene blue dye in an aqueous medium

Samie Yaseen Sharaf Zeebaree [a,*], Aymn Yaseen Sharaf Zeebaree [a], Osama Ismail Haji Zebari [b], Ali Yassin Sharaf Zebari [c]

[a] Dept. of Medical Laboratory Technology, Shekhan Technical College of Health, Duhok Polytechnic University, Kurdistan Region, Iraq
[b] Medical Biochemical Analysis Department, College of Health Technology, Cihan University-Erbil, Kurdistan Region, Iraq
[c] Laboratory Department, Shekhan General Hospital, Ministry of Health, Iraq

ARTICLE INFO

Keywords:
Copper nanoparticles
Malva sylvestris
Methylene blue
Removal

ABSTRACT

Copper nanoparticles have obtained due to the green process in a one-pot reaction at ambient temperature using *Malva Sylvesteris* leaves extract. The plant extract has used as a reducing and capping agent, providing stability and avoiding oxidation of synthesized copper nanoparticles for more than eight months. Many techniques have exploited for the investigation of optical and physicochemical properties of copper nanoparticles. UV-VIS spectroscopy showed two bands at different locations for the extract and nanoparticles at 340 and 390 nm, respectively. Fourier transform infrared spectroscopy confirmed the role of bioactive materials in the plant extract as a reducing and capping agent. X-ray diffraction tool affirmed the crystalline nature of fabricated copper nanoparticles at average (20 nm) and showed a centred cubic structure. Field emission scanning electron microscope (FESEM) chart illustrated the roughly spherical shape of distributed copper nanoparticles. The copper nanoparticles showed high-efficiency removal of methylene blue dye in water samples.

1. Introduction

Population growth and rising demand for drinking water worldwide attract scientists and researchers to find a rapid solution to these challenges. Recently, water pollution becomes one of the most global issues due to the rising of pollutant resources everywhere [1]. Many contaminants, such as toxic dyes [2], oil derivatives, pesticides, herbicides [3], heavy metals, and plastics, affect water quality due to undegradable by microorganisms (bacteria and fungi) [4]. Dyes and tinctures have extensive utilization in the industrial process, such as pharmaceutical [5], foodstuff [6], cosmetic [7], plastics [8], and papers [9]. The broad usage of dyes led to countless environmental issues such as soil and water contamination and poisoning beneficial organisms in the aquatic system [10,11]. Scientists' efforts have been directed to minimize these issues by developing efficient methods for water remediation and decreasing pollutants. Numerous techniques have been used for water treatment involved chemical oxidation, adsorption, chemical precipitation/coagulation, ion exchange, and chemical precipitation. Most of them observed many drawbacks, such as requiring high temperatures, using harmful chemicals, time-consuming, and high costing [12]. Nanotechnology holds considerable promise to provide the best feasible methods to treat water pollution due to its remarkable properties and high efficiency [13]. Recently, nanomaterial substances have been exploited for solving the current water problems using nano sorbent [14,15], bioactive nanoparticles [16], nanocatalyst [17], and nanofiber [18]. Nanomaterials possess different behaviour than bulk materials because of high surface area to volume and a broad range of physicochemical properties [19]. It considered a unique implement for separation and active media for water purification [20]. Many approaches have been invented to fabricate nanomaterials, for instance, chemical vapour deposition, colloidal dispersion, sol gel, hydrothermal route, and microemulsion. Although these methods produce distinctive nanomaterials, it suffers from solvents-consuming, high costing, and environmentally harmful [21]. Therefore, developing an alternative approach was highly recommended, such as the green synthesis of nanoparticles. The plant extract has attracted scientists' attention due to

* Corresponding author.
E-mail addresses: samie.yasin@dpu.edu.krd (S.Y. Sharaf Zeebaree), aemanzebari2002@gmail.com (A.Y. Sharaf Zeebaree), osama.haji@cihanuniversity.edu.iq (O.I. Haji Zebari), ali.zebari8787@gmail.com (A.Y. Sharaf Zebari).

https://doi.org/10.1016/j.crgsc.2021.100103
Received 27 December 2020; Received in revised form 1 March 2021; Accepted 23 April 2021
Available online 14 May 2021

its possessing many bioactive compounds, which used as the best alternative to conventional nanomaterial production processes [22]. *Malva sylvestris,* commonly known as mallow is a famous plant in the medicinal field. It contains active biochemical compositions, such as anthocyanins, leucoanthocyanins, flavonoid glycosides, polysaccharides mucilaginous, and polyphenol [23]. Bioactive components of plant considered as green capping and reducing agents. However, it was used to reduce metallic ions and the synthesis of metallic nanoparticles [24]. Among all noble metals, copper has an attractive feature due to its availability, low cost, unique catalytic properties [25]. Copper nanostructure saw vast applications, such as catalyst [26], antibacterial agent [27], anti-cancer [28], sensor [29], and adsorbent [30]. Many studies have conducted the fabrication of metal nanoparticles and evaluate their capacity as an adsorbent catalyst for removing toxic dyes. For instance, Joshi et al. [31] prepared a Fe3O4@AC nanoparticles for dye removal from simulated wastewater, while Kale et al. [32] synthesized a NiNPs by polyvinyl pyrrolidone (PVP) as NPs stabilizer, whilst Sharma et al. [33] prepared FeNPs immobilized by Agrobacterium fabrum biomass as biosorbent for removal of MB dye from aqueous solution, whereas Afkhami et al. [34] prepared maghemite nanoparticles as adsorptive material for removal of Congo red as carcinogenic dye for textile from aqueous solutions. Most of the mentioned methods observed of long time adsorption, using complex apparatus, high consuming of some toxic surfactant, and required high pH solution. So, the previous dilemmas were tackled by preparing green nanoparticles catalysts exploiting the biological components including plants as sustainable, environmentally friendly source as an active catalyst for removing of dyes with higher efficiency and effectiveness than previous counterparts [35].

This study aims to synthesise copper nanoparticles in a one-pot process. a green and eco-friendly approach without adding any harmful chemicals, undesirable solvents, and surfactant has been employed to fabricate copper nanoparticles. *Malva Sylvesteris* leaf extract (MSLE) used as a reducing and stabilizing agent to control the shape and size of CuNPs. According to the standard JCPDS (No. 48-1548) data, Spectrum techniques confirmed the shape and diameter of formed nanoparticles. MCuNPs observed high removal efficiency of methylene blue dye in an aqueous solution and in a short time.

2. Materials and methods

A healthy green *Malva Sylvesteris* Leaves were collected from the Charboot village-Zeebar area/Duhok-Kurdistan region of Iraq during the month of April 2020. Copper (II) sulfate anhydrase ($CuSO_4$ 99.5% purity, M.wt = 159.6086 g/mol, CAS number: 7758-99-8) and Methylene blue dye ($C_{16}H_{18}ClN_3S$, M.wt = 319,86 g/mol, CAS number [61−73−4]) was purchased from Scharlau lab Spanish Co. without further treatment.

2.1. Preparation of Malva Sylvesteris leaves extract (MSLE)

Malva Sylvesteris leaves were collected and washed in distilled water for 5 min then dried in the sunlight for 24 h. The dry leaves (10 g) were crushed in the mortar to a fine powder and dissolved in 100 ml deionized water in a conical flask 250 ml, then heated at 60 °C for 1 h. Next, the mixture solution was filtered by a filter paper three times to remove insoluble fractions and macromolecules to obtain a slight brown solution of MSLE. The filtrate solution of MSLE was stored in the refrigerator 2 °C to be used in the next step as a reducing, capping, and stabilizing agent for synthesizing copper nanoparticles.

2.2. Green fabrication of copper nanoparticles (MCuNPs)

Green fabrication of copper nanoparticles (MCuNPs) was performed in one pot by mixing 25 ml of prepared copper sulfate anhydrous solution (0.1 M) with 75 ml of MSLE in the conical flask of 250 ml stirring for 2 h. After that, a green suspension is reported, indicating the formation of MCuNPs. Next, the suspension centrifuged at 4000 rpm for 5 min to get nano precipitate, then collected and washed several times with distilled water and left over 24 h to dry. The excess of obtained green suspension was stored at room temperature for different period times to study nanoparticles stability [36].

2.3. pH at point of zero charge

The pH point of zero charge (pHpzc) was determined according to the previously reported procedure [37]. A weighed amount (0.1 g) of MCuNPs was added to 50 ml of 0.1 M NaCl with predetermined pH in a 250-ml conical flask. The resultant solution's pH was adjusted between pH 2 and 10 with either 0.1 M NaOH or HCl. The conical flasks were sealed and shaken in an orbital shaker for 24 h, after which the final pH values were measured. The difference between the initial and final pH was calculated and plotted against the initial pH. pHpzc was obtained from the point of intersection with the pH axis.

2.4. Characterization techniques

The wavelength of the stabilized color of MCuNPs was measured via Ultra Violet-Visible (UV–Vis) spectrophotometer (Mod.220v -JENESA 752 N, Iraq) scanning 320–750 nm. The oxidation state of the elements compositions was analyzed using AXIS ULTA-AXIS 165 X-ray Photoelectron Spectrometer (XPS). The possible biofunctional groups of MSLE components and MCuNPs precipitate were characterized by Fourier transform infrared (FT-IR) spectroscopy (Nicolet 6700, ATR, Iran) in the scanning range 4000–500 cm^{-1} with a resolution at 4 cm^{-1}. The predicted shape structure of prepared MCuNPs was estimated by X-ray diffractometer (Philips X'Pert PRO equipped with line detector) and CuKα (l = 1.540 Å) radiation in a 2θ configuration at the range of 10–80° with scanning rate was 0.026/min and operating at a voltage of 40 kV and a current of 30 mA. The crystalline nature and elements ratios of MCuNPs structure were observed via field emission scanning electron micrographs (FESEM, TESCAN BRNO-Mira3 LMU, japan) at an accelerating voltage of 10 kV, equipped with energy dispersion spectroscopy analysis. High resolution-transmission electron microscopy (HR-TEM) measurement and mean particle size calculated were performed for MCuNPs in an JEOL JEM 2100, japan operating at 200 kV, with a resolution point of 2.04 nm. The mean particle size and zeta potential of prepared MCuNPs were measured using Malvern Zetasizer-Nano analyzer (Malvern instrument Inc., UK) at the temperature of 25 °C.

2.5. Removal test

The efficiency of MCuNPs was evaluated against removing methylene blue dye (MB) in an aqueous solution. The process has been performed by mixing of 0.02 g of MCuNPs with 5 ml 10 ppm of MB dye solution in the 10 ml vial with stirring at ambient temperature and room light for 20 min to ensure the process of dye elimination. The sample was withdrawn from the vial for a fixed interval of time to screen the dye removal by using a spectrophotometer device. The following equation (1) has been used to calculate the percentage removal of methylene blue (MB) dye in the aqueous solution:

$$\text{Removal percentage } \% = [\, C_o - C \,/\, C_o \times 100] \quad (1)$$

Where *Co* is the initial concentration of MB dye, *C* is the MB dye concentration (mg/L) after various time.

3. Results and discussion

3.1. MSLE bio-compositions and their supported mechanism with XPs analysis in MCuNPs formation

The known *Malva sylvestris* plant (Fig. 1a) grows wildly in all temperate regions of Asia, Europe, North Africa, and America, making it

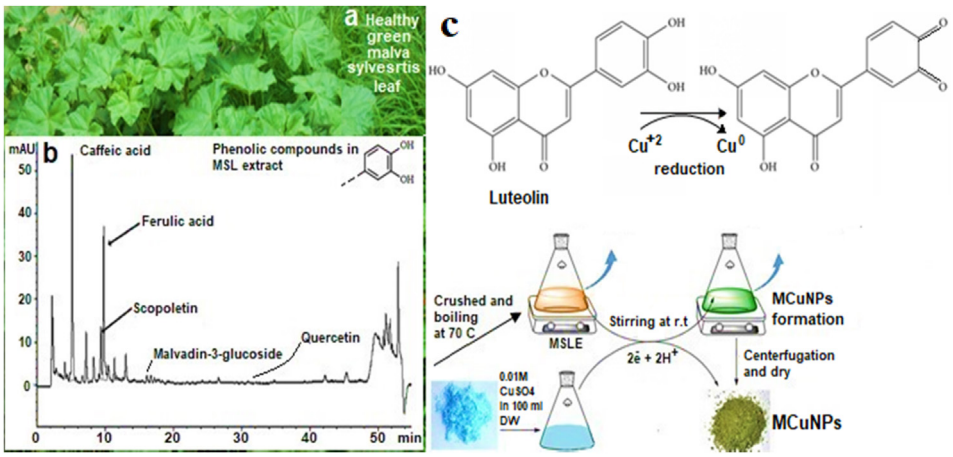

Fig. 1. Healthy MSL (a) MSLE HPLC analysis finger print (b) Proposed mechanism of MCuNPs synthesized (c).

an available usage source in many scientific applications. In the medical application, *Malva sylvestris* used as a herbal plant as an inflammatory, antibacterial, anticancer, and antioxidant due to its active bio compositions [38]. The high performance liquid chromatographic (HPLC) analysis of Malva's leaf extract has been prepared by the Ahmed and Muhammad report (Fig. 1b) [39,40]. It is revealed that it contains a wide spectrum of bio phenolic compounds such as caffeic acid, ferulic acid, malvadin-*3*-glucoside, quercetin, scopoletin, quercetin-*3*-*D*-glucoside, rosmarinic acid, *n*-coumaric acid, epicatechine, rutin, ellagic acid, apigenin, luteolin, epicatechine, chlorogenic acid and hyperoside that possessed high antioxidant activity. This efficiency is attributed to the hydroxyl groups of these compounds. Furthermore, play a significant role in the redox process in which act as an electrons donor in the metal reduction process. Owing to its high availability percentage among other Malva extract components, the reduction mechanism proposed that Luteolin (one of quercetin derivatives) is responsible for forming MCuMPs, as illustrated in Fig. 1c. The high reducing ability of these bio components confirmed the green application of *M. sylvestris* leaf extract as a perfect source for the fabrication of CuNPs with high yield [41].

Moreover, the XPs analysis for as-prepared MCuNPs has been conducted to confirm the green reduction process. The XPs spectrum survey of Cu (Fig. 2a) revealed excellent photoelectron peaks for orbitals states of Cu [Cu2p, Cu3s, Cu3p, and its Cu LMM Auger]. The high-resolution XPS spectra (Fig. 2b) showed sharp-broad fitting peaks located around 933.1, 935.2 eV, 951.5 and 953.4, which refer to the Cu 2p, Cu $2p_{3/2}$, Cu $2p_{1/2}$, respectively. These obtained resultants are following literature results [42] in the formation of green CuNPs. Besides, the gap between each Cu $2p_{1/2}$ and Cu $2p_{3/2}$ at 19.8 eV, is another evidence that matches the standard value of 20.0 eV for the prepared CuO [43]. Finally, the appearance of two shake-up satellite peaks at 942.9 and 962.7 eV is another evidence of an open 3d9 shell corresponding with the state of Cu+ in the formation of MCuNPs. No appearance of impurities metal on the surface of the NPs is an indication of the cleanesty preparing of MCuNPs.

3.2. Ultra Violet-Visible (UV–Vis) measurement

The appearance of the green colloidal solution that resulted from the addition of brown MSLE solution to the colorless copper sulfate is indicative of the MCuNPs formation (Fig. 3a). This changing in colors has been studied by UV–Vis spectroscopy measurement. The slight brown MSLE solution showed a broad absorption band at 287 nm, whereas green MCuNPs revealed two bands at 340 nm and 535 nm respectively. Peak shown at 340 nm is attributed to the nuclei structure of flavonoids of MSL components, whereas the maximum absorbance of green synthesized MCuNPs at 535 nm return to surface Plasmon absorption. This due to the collective oscillation of free electron conduction band, which is excited by the incident electromagnetic radiation [44]. This kind of resonance is seen when the incident light wavelength far exceeds the particle diameter. The bio-prepared MCuNPs revealed good bandgap energy at 2.52 eV through tauc plot (Fig. 3b), indicating good interband transitions of core electrons. The nanoparticle structures' optical features depend on their sizes, shapes, and stability in the surrounding environment. Thus, the color constancy and wavelength (Fig. 3c) indicates that the nanoparticles have been synthesized with relatively stable sizes.

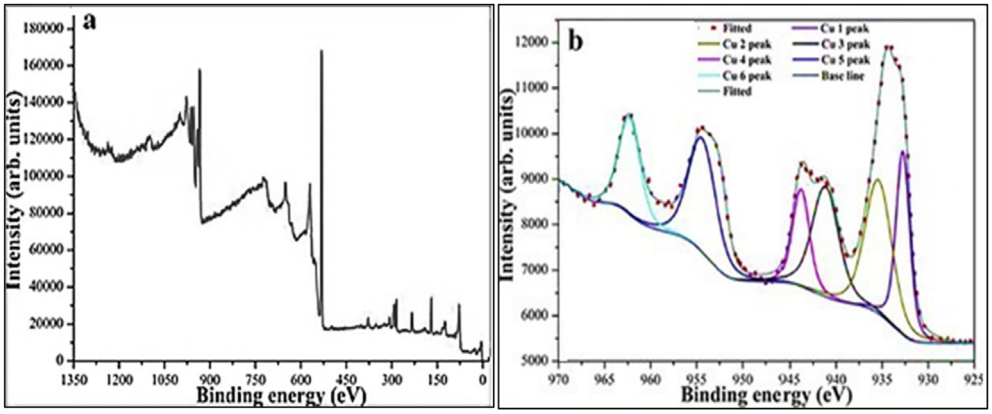

Fig. 2. (a–b) XPs analysis of the MCuNPs.

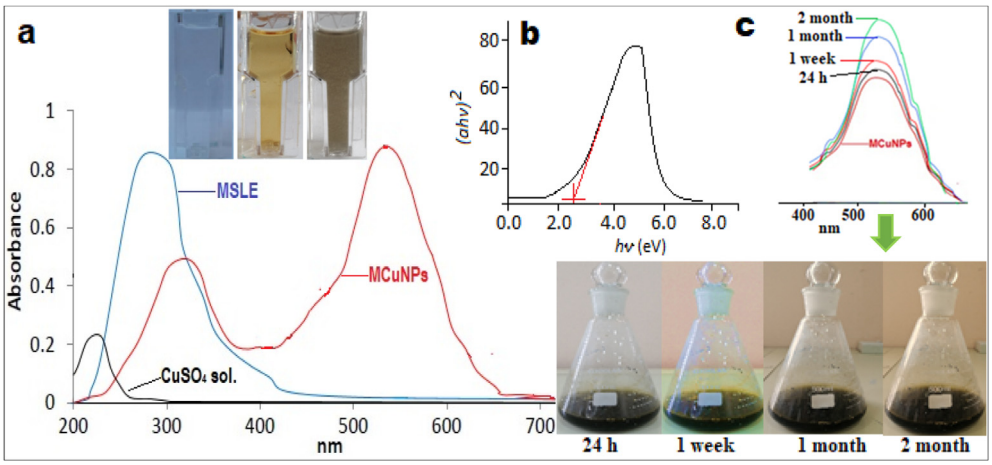

Fig. 3. UV–Vis measurement of (a) MSLE, $CuSO_4$ sol. and MCuNPs, (b) Band gap energy of MCuNPs (c) MCuNPs wavelength stability at the various time illustrated with images.

3.3. Fourier transform-infrared radiation (FT-IR) analysis

FT-IR analysis was performed to reveal the bio-functional groups of *Malva sylvesteris* leaf extract (Fig. 4a) responsible for synthesizing MCuNPs (Fig. 4b). Fig. 4a of MSLE showed robust broadband at 3447 cm^{-1} is attributed to the hydroxyl group (O–H) of the phenolic compounds, which reduced to 3422 cm^{-1} when the CuNPs synthesized (Fig. 4b). This transformation is due to the occurrence of conjugation in the hydroxyl groups responsible for the reduction and formation of copper nanoparticles. Also, the both FTIR spectrum showed significant ranges at 2928 cm^{-1}, 2850 cm^{-1}, attributed to the expansion bands of the CH_2 and C–H alkane groups which reduced to 2924 cm^{-1} and 2841 cm^{-1} in the prepared CuNPs. Both figures showed a long sharp band at 1540 cm^{-1} which was attributed to the C═C group vibrations for aromatic phenol ring. The emergence of a sharp peak at 1701 cm^{-1} in *Malva sylvesteris* leaf extract which increased to 1715 cm^{-1} attributed to the new carbonyl (C═O) group expansion vibrations of ketone that associated with C═C group in flavone compound that responsible on the formation and stabilizing M-CuNPs. Appearance of special peaks located in the range 698–1449 cm^{-1} are is attributable to the O–H phenolic group, C–N expansion vibrations of aliphatic and aromatic amines as well as C–H bending vibration in the polysaccharide compounds. Fig. 1b extremely showed a major peak at 525 cm^{-1} which is attributed to the Cu–O band fo prepared M-CuNPs. The shift in these bands clearly indicates the responsible of phenolic compounds in *Malva sylvesteris* leaf extract done in well in the formation, stabilization and coating of M-CuNPs. These results obtained analysis above are welly in agreement with our previously published report [44].

3.4. X-ray diffraction (XRD) analysis

The crystalline nature of prepared MCuNPs has been estimated by XRD analysis (Fig. 5) which gave characteristic peaks at positions $2\theta = 38.31^{\circ}$, 47.92° and 66.12°, which possessed indices of 111, 200 and 220, where identically to the characteristic of the face-centred cubic structure (fccs) and which in consistence with the standard JCPDS (No. 48-1548) data. No other impurity peaks shown except Cu were observed in the XRD spectrum indicating the high crystalline purity of MCuNPs and with small sizes. The average crystallite size of the M-CuNPs has been calculated by Debye–Scherrer's formula $\boldsymbol{(D = k\lambda/\beta\cos\theta)}$, where parameters D, k, λ, β and 2θ refer to the particle size (nm), constant equal to 0.9, the wavelength of X-ray radiation (0.15418 nm), the full-width at half maximum (FWHM) of the peak and the Bragg angle (degree), respectively. The formula showed that the average size of the crystals formed ranged between 17 and 25 nm.

3.5. Morphological characterization of MCuNPs

Performing FESEM and HR-TEM micro analysis to detect the formed nanoparticle structure is extremely required for their contribution to describing the nature of the particles involved in the adsorption process. The FE-SEM image showed that green copper nanoparticles formed in a spherical agglomerates shape due to the MSL extract's oily nature (Fig. 6a). The FESEM micrograph recorded the formation of MCuNPs with fine sizes ranged 27–31 nm, indicating the effectiveness of biosynthesis. The purity of prepared green MCuNPs has been estimated by measuring their components using EDS analysis. EDS spectrum (Fig. 6b) showed excellent elements compositions for carbon (C), copper (Cu) and oxygen (O) with weights 45.2%, 37.5% and 17.4%, respectively. No appearance of other elements is further evidence of the purity of bio preparation. More analyzing, the crystalline nature of the MCuNPs was verified more closely by HR-TEM micrograph, which showed the formation of agglomerated and uniform spherical nanocrystal with sizes ranged 23–27 nm (Fig. 6c). HR-TEM analysis clearly supported the FE-SEM image, as it revealed that the reason for the nanoparticles aggregating was due to the role of bio-components that acted as a reducing and binding agent. Fig. 6d shows the calculated size distribution of the prepared MCuNPs that ranged from 22 to 25 nm. Another proof, Selected Area Electron Diffraction (SAED) measurement (Fig. 6e), showed intermittent dots in the concentric circles, which is another indication of the crystalline nature of the fabricated MCuNPs. This case is interpreted that the prepared nanoparticles may exhibit excellent dispersion within the bio-reduced aqueous solution, even at the macroscopic scale.

3.6. Zeta potential and size distribution measurements by dynamic light scattering (DLS)

Performing DLS analysis was used to estimate the size and surface charge of the prepared MCuNPs, as shown in Fig. 7a–b. Zeta potential analysis revealed that the prepared MCuNPs possessed a high negative charge of −25.2 mV with a zeta deflection at 8.21 mV (Fig. 7a) with a polydispersity index value of 1.00. This high negative value of zeta potential attributed to binding force among the agglomerated nanoparticles [45]. Fig. 7b shows that the green synthesized MCuNPs have average particle size distribution of 45 nm. This fine size of MCuNPs is ascribed to the biomolecules layer covering the surface of nanoparticles. Many reports have suggested that the size and charge distribution of prepared NPs by biomolecules enhance the capabilities of the CuNPs in the adsorption of dyes polluted [46].

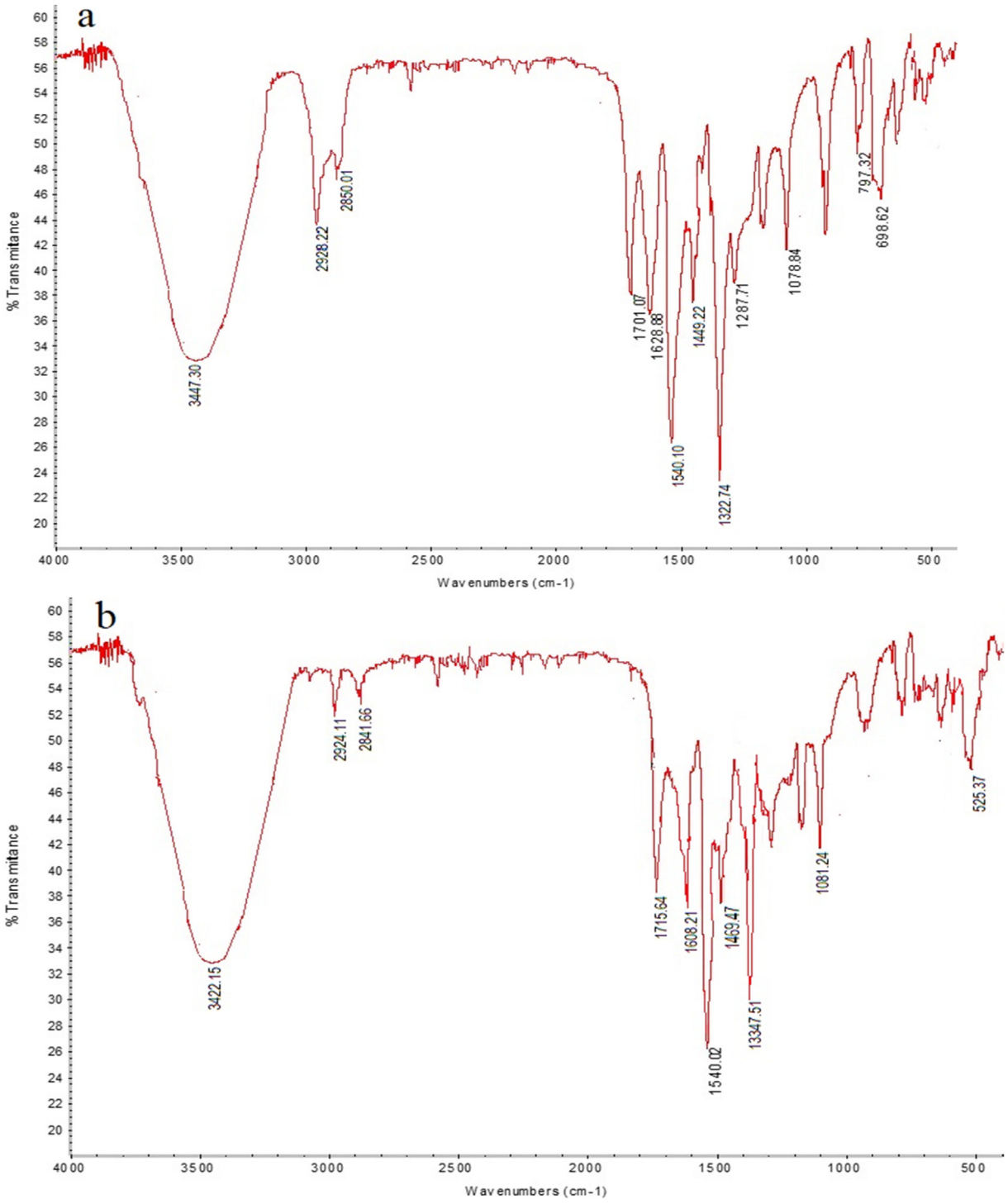

Fig. 4. FT-IR analysis of (a) MLSE and (b) M-CuNPs.

3.7. Removal of MB dye by MCuNPs

The fabricated copper nanoparticles' performance as an effective catalyst for removing methylene blue dye (MB) has been tested in an aqueous solution. The process was evaluated in the presence and absence of copper nanoparticles. The quantity of catalyst has been chosen after evaluating the efficiency of the minimum amount of catalyst. The procedure was conducted by adding 0.02 g of MCuNPs to 5 ml of the MB dye solution (10 ppm, pH = 6). The mixture of the reaction was stirred magnetically thoroughly at continuous times in room light. A portion (2 ml) was taken out and measured by UV–vis spectrophotometer at each 5 min periods. It was observed that the absorbance of the blue colour solution diminished gradually and converted to colourless as time passed. This can be justified that the dye molecules have adsorbed on the nanoparticles' surface, as shown in Fig. 8a. The disappearing of dye colour was followed, as illustrated in Fig. 8b. It has been reported that the equilibrium between the dye and active sites of the catalyst occurred after 20 min. The experiment has been performed in a dark place in order to affirm the efficiency of the process. It has been reported that the removal of dye has proceeded effectively even in the dark place. However, the catalyst activity of the MCuNPs in compared with the solution without the catalyst were investigated. It was clear that, without adding

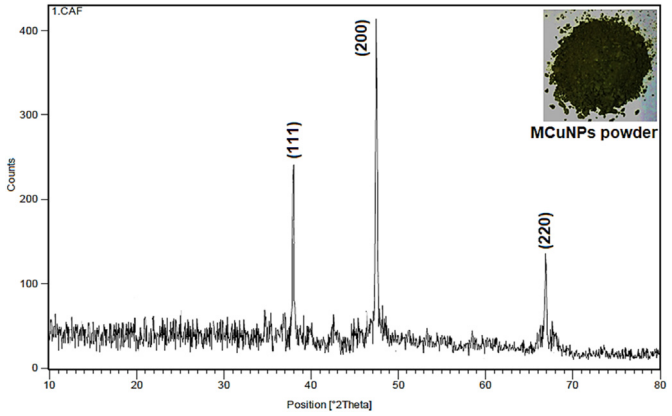

Fig. 5. XRD analysis spectrum of the MCuNPs synthesized.

the catalyst, the absorption value of MB dye was steady at the same time, while the green copper nanoparticles showed high adsorption of dye. The colour removal process of MB dye by green copper nanoparticles was significantly higher, reaching almost 92.1% decolourisation. These obtained results and high efficiency of MCuNPs in higher dye decomposition are compared with the other related research studies using the green and non-green methods as a dye removal agent (Table 1). The data indicate that the prepared MCuPs showed a higher removal capacity of MB with less time and lower irradiation intensity compared to the capacity features of CuNPs in other studies (green and non-green methods). This high-fast dye removal is attributed to the high surface area of achieved CuNPs decorated by bio-compositions of *Malva* leaves extract (see Fig. 9).

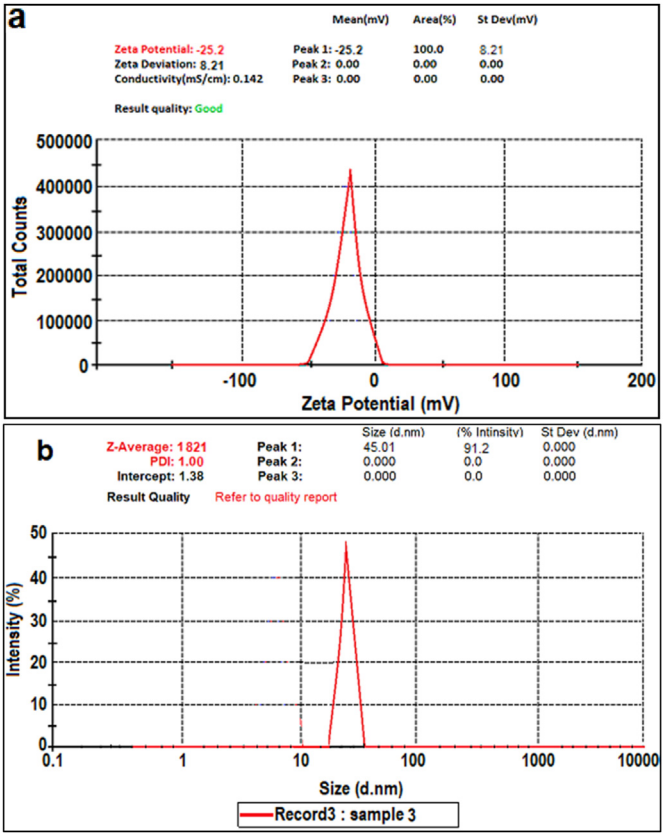

Fig. 7. Zeta potential (a) and size distribution (b) of the MCuNPs.

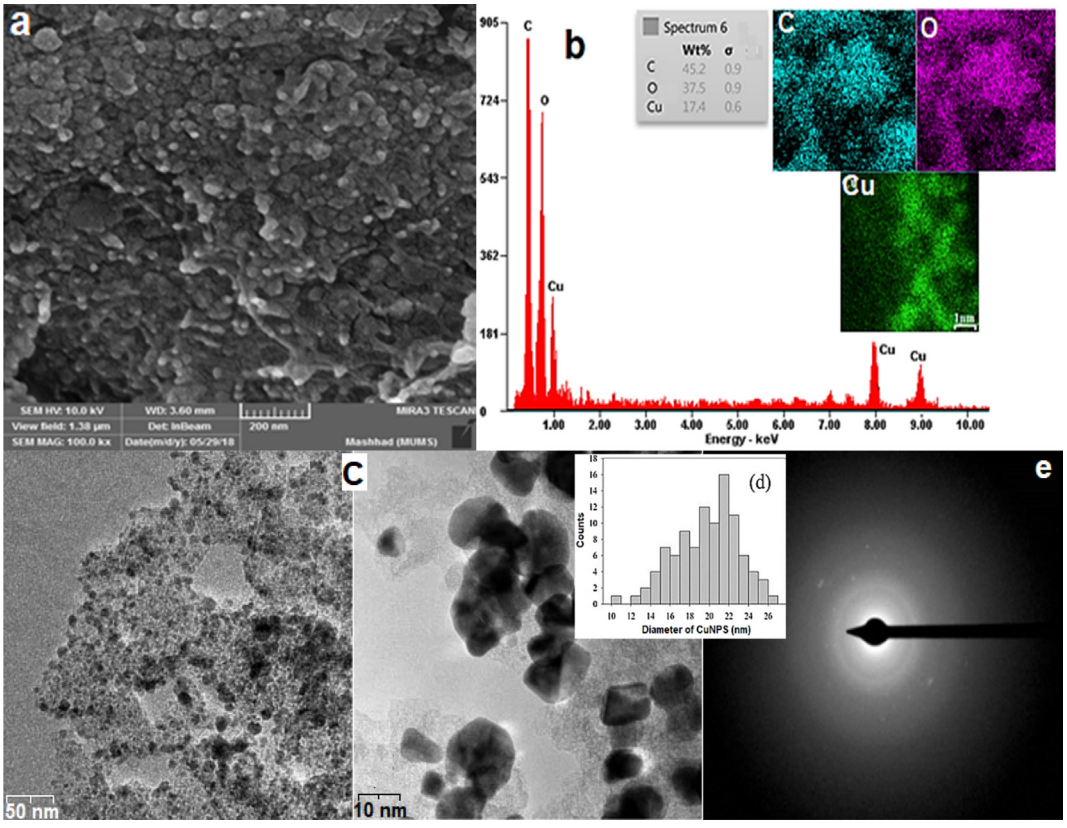

Fig. 6. MCuNPs diagnosis by: FESEM (a), EDS (b), HR-TEM in two zoom (c), size diameter (d), MCuNPs diameter sizes, SADE (e).

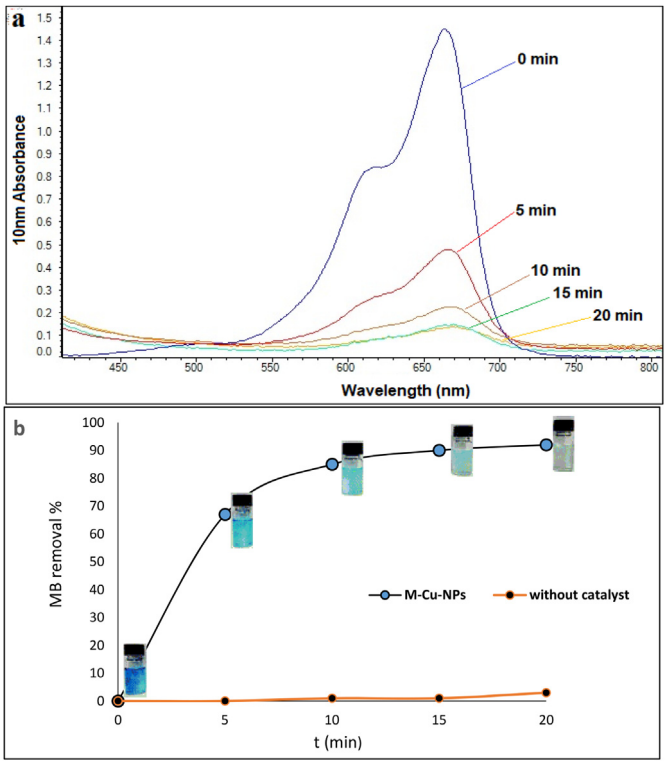

Fig. 8. (a) UV–vis bands of MB dye adsorption at various time, (b) MB dye removal % percentage.

3.8. Kinetic analysis

In order to calculate the order of reaction, two standard kinetic equations have been applied to investigate the mechanism adsorption of MB dye on the surface of the catalyst, i.e, the pseudo-first-order equation (2) and pseudo-second-order equation (3) model.

$$ln(qe - qt) = ln\ qe - k_1\ t \quad (2)$$

where qe = (mg/g) the amount of adsorbed dye at equilibrium, qt = (mg/g) the amount of adsorbed dye at time t (min)

$$\frac{1}{q_t} = \frac{1}{q_e} + \frac{1}{k_2 q_t} \quad (3)$$

Methylene blue dye was classified as a cationic dye, which belongs to a widespread category of dyes [55]. According to Zeta potential analysis that showed the nanoparticles synthesized using plant leave extract have a negative charge on the surface of copper nanoparticles. This explains the interaction process between the nanoparticle's negative charge surface and positive charge molecules of methylene blue dye. Additionally, the kinetic parameters have calculated, which explain the value of regression coefficients for both pseudo-first order and second order (Table 2). The R^2 value for pseudo-first order was 0.987 and for pseudo-second order was 0.995 respectively.

3.9. Adsorption isotherm study

Matching isotherm data with the various model is the main thought in appointing a suitable model for developing water treatment station. Langmuir model equation (4) was applied to equilibrium data achieved from adsorption of methylene blue dye onto the surface of MCuNPs.

$$\frac{C_e}{q_e} = \frac{1}{Q_0 k_l} + \frac{C_e}{Q_0} \quad (4)$$

C_e = Equilibrium concentration of MB (mg/L).
q_e = Value of MB adsorbed on the MCuNPs (mg/g).
Q_0 and k_l = Maximum adsorption capacity (mg/g) and Langmuir constant, respectively.

The R^2 value indicated that the adsorption process was fine fitted with the Langmuir isotherm equation, which supposes the regular activity distribution of adsorbent as a monolayer on the adsorbents' surface [56] (Fig. 10a).

The Freundlich isotherm could be expressed as the following (equation (5)):

$$\log q_e = \log k_f + \frac{1}{n} + \log C_e \quad (5)$$

k (mg/g) and n is Freundlich constant. k_f show the sorbent capacity while n explain the nature of the adsorption process. By plotting log q_e vs. log C_e (Fig. 10b), respectively, it is possible to obtain the value of 1/n and k_f from the slope and intercept of the plot. The calculated values of the Langmuir and Freundlich model equation were observed in Table 3. It clear that the removal of MB dye by MCuNPs was well fitted with the Langmuir model.

3.10. pH at point of zero charge (pHpzc)

The treatment efficiency of MCuNPs revealed remarkable successful against the removal of MB dye due to considerable adsorption of

Table 1
Comparison of MCuNPs with other related reports in MB degradation.

Adsorbent	Dye concentration	Irradiation light source	Recorded time (min) & removal%	Reference
Green method				
Labeo rohita-CuONPs	10 mg/l	Sunlight.	135 min, 96%	[35]
CuONPs- *Aloe Vera*	1000 mg/l	Room light	210min, 98%	[47]
Rheum palmatum-CuO NPs	10 mg/l	Room light	60 min, 99%	[48]
Aloe Vera-CuONPs	10 mg/l	UV-Xe lamp 100 W	47 min, 70%	[49]
CuO/PET nanocomposite	10 mg/l	UV lamp 10 W	30 min, 99%	[50]
Malva-CuONPs	10 mg/l	Room light	20 min, 92.1%	this work
Non-green method				
[a] CuO-NPs	5×10^{-3} M	Sunlight	50 min, 85%	[51]
[b] CuO-NPs	10 mg/l	Room light	100 min, 80%	[52]
[c] CuO-NPs	15 mg/l	Illuminated UV source (365 nm)	180 min, 89%	[53]
[d] CuO-NPs	2×10^{-5} mol/l	Sunlight	120 min, 93%	[54]
MCuOPNs	10 mg/l	Room light	20 min, 92.1%	this work

[a] Sol-gel method.
[b] Co-precipitate.
[c] Hydrothermal method.
[d] Electrochemical synthesis.

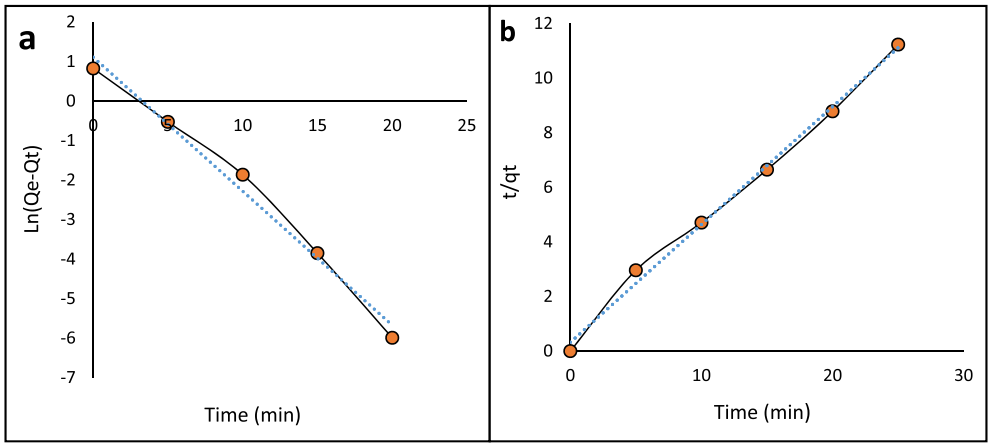

Fig. 9. Pseudo-first order (a) and pseudo-second-order (b) plots of MB removal process.

Table 2
Kinetic parameters of pseudo-first-order and pseudo-second-order.

pseudo-first-order			pseudo-second-order		
k_1 (min^{-1})	q_e	R^2	K_2 (min^{-1})	q_e	R^2
0.0135	3.00	0.987	0.575	2.31	0.995

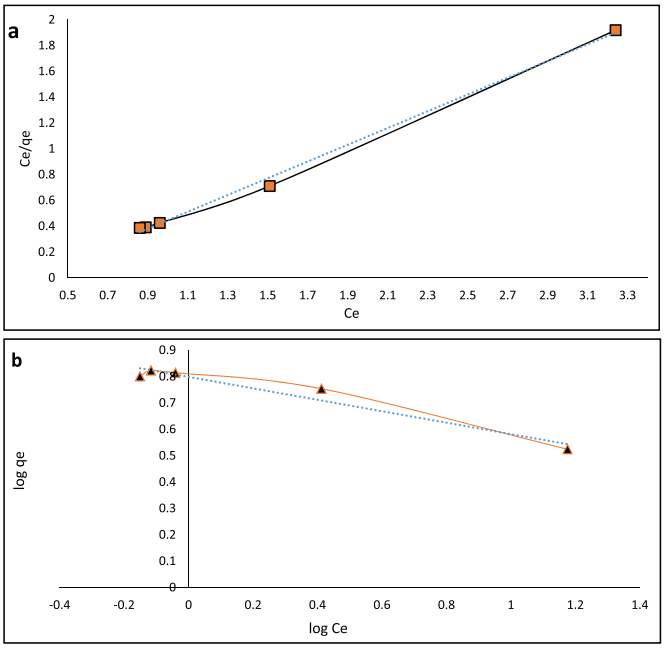

Fig. 10. Application of Langmuir model equation (a) and Freundlich isothermal equation (b).

Table 3
Isotherm parameters of MB adsorption on MCuNPs (pH = 6.5, $Conc._{adsorbent}$ = g/L, T = 298 K).

Langmuir Isotherm			Freundlich Isotherm		
Q_0	k_l	R^2	n	K_f	R^2
4.97	0.310	0.996	4.60	6.28	0.94

positively charged MB dye by the surface of negatively charged MCuNPs. The phenomena of dye removal depend upon the zero point charge of MCuNPs. The pH at point of zero charge (pHpzc) of MCuNPs was determined by plotting the final pH vs initial pH after 48 h (Fig. 11). The

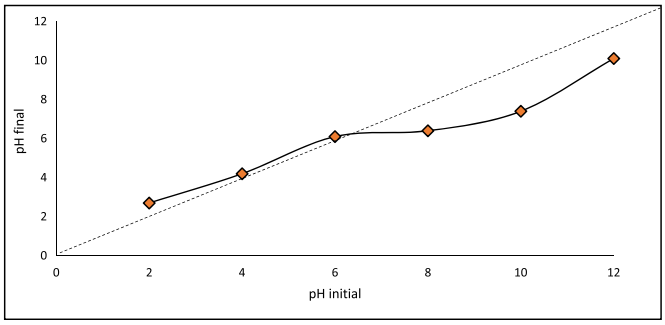

Fig. 11. Calculation the pHpzc of MCuNPs.

pHpzc of the MCuNPs was 6.1. According to the calculated pHzpc value, if the pH solution is higher than pHzpc the surface of MCuNPs is became negatively charged. While at a lower pH solution, the surface becomes positively charged. In the present study, the solution pH showed a value (pH = 7.5) greater than pHpzc, so the surface becomes negatively charged, favouring the uptake of positively charged MB dye. This obtained result is consistent with previous reports [57].

3.11. Influence of initial dye concentration and pH medium on removal of MB dye

The efficiency of dye removal was explored by investigating the effect of the initial dye concentration on the adsorption process. Various concentrations of MB dye were prepared and ranged between 10 and 200 (mg/L) and fixed amount of MCuNPs (0.02 mg). Fig. 12a shows that, at low initial concentration, the adsorbent shows high removal percentage, While the removal effectiveness has decreased by increasing the initial concentration of MB dye. This can be attributed to the fill of the active monolayer sites on the surface of the adsorbent [58]. On the other hand, the influence of the acidity and basicity on the removal of MB dye has been studied. Different solution of MB dye has been prepared with varied pH ranged between (2-12) using 0.1 M HCl, and NaOH. Fig. 12b illustrates that, the removal efficiency saw raising by increasing the pH value of the mixture, and peaked at pH 7.5. After that the dye removal percentage has fallen gradually by increasing the basicity of the solution. This can be described on the basis of the electrostatic attraction between the cationic molecules of MB dye and anionic surface of the adsorbent which is the main force responsible for the adsorption process [59]. Therefore, pH 7.5 is selected as the optimum medium for further investigation (pH).

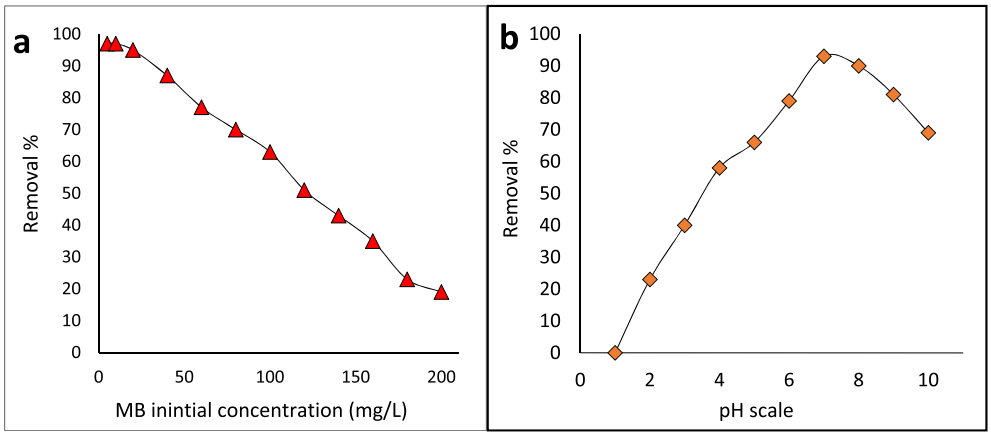

Fig. 12. The influence of the initial concentration (a) and pH (b) on MB dye removal.

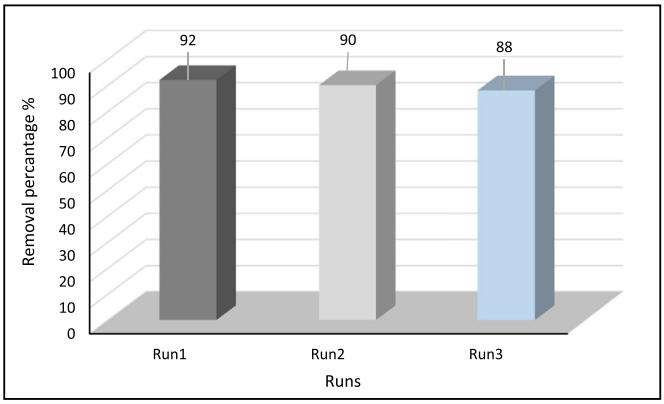

Fig. 13. Recycling of the MCuNPs in the MB removal process.

3.12. MCuNPs reusability and their efficiency against MB dye

The quality of the MCuNPs catalyst has been studied by checking the recyclability of the MCuNPs. Further, the ability to reusing it again against the MB dye at the same conditions. After completing the first run, the MCuNPs were recovered by centrifuges process and simple filtration and were washed repeatedly with distilled water and dried at 50 °C in a hot air oven then dried. After that, two more runs of the reusable catalyst were also used against MB dye, and it was found that they occurred without appreciable loss of catalytic activity (Fig. 13). A simple deviation of the catalyst efficiency was observed among the first and third cycles due to the slight loss of the MCuNPs catalyst during the filtration process. According to obtained results, it seems possible that the recovery can be successfully achieved more than once with high efficiency, indicates to the MCuNPs effectiveness.

4. Conclusion

In the current work, copper nanoparticles (MCuNPs) have been successfully synthesized via a green, clean, low-cost and environmentally friendly method using leaves extract of *Malva sylvestris* plant as a reducing and stabilizing agent. Spectrums examination illustrated that the spherical, high surface area, well dispersed and size range between 15 and 25 nm of MCuNPs nanoparticles had been obtained. The kinetic results showed that the process of dye removing was followed pseudo-second reaction R^2 (0.995). The equilibrium data exhibited that the maximum adsorption process was fitted with Langmuir model equation R^2 (0.996). Furthermore, other parameters were reported in this study: PH of medium, initial concentration of dye, and removal time (pH = 7.5, 10 ppm, 20 min), respectively. The efficiency of MCuNPs to remove the methylene blue (MB) dye was very high compared to the literature. Additionally, MCuNPs eliminate MB dye species in an aqueous medium at a high percentage 92% in a short time. This study could pave the way to some possible application of nanoparticle for the purification of contaminant water.

CRediT authorship contribution statement

Samie Yaseen Sharaf Zeebaree: Conceptualization, Writing – original draft. **Aymn Yaseen Sharaf Zeebaree:** Conceptualization, Writing – review & editing. **Osama Ismail Haji Zebari:** Writing – review & editing. **Ali Yassin Sharaf Zebari:** Writing – review & editing.

Declaration of competing interest

The authors declare that they have no known Conflict of Interest interests or personal relationships that could have appeared to influence the work reported in this paper.

References

[1] A. Boretti, L. Rosa, Reassessing the projections of the world water development report, Npj Clean Water 2 (2019) 1–6, https://doi.org/10.1038/s41545-019-0039-9.
[2] L.M. Pandey Ravi, Enhanced adsorption capacity of designed bentonite and alginate beads for the effective removal of methylene blue, Appl. Clay Sci. 169 (2019) 102–111, https://doi.org/10.1016/j.clay.2018.12.019.
[3] A. Jawed, V. Saxena, L.M. Pandey, Engineered nanomaterials and their surface functionalization for the removal of heavy metals: a review, J. Water Process Eng. 33 (2020) 101009, https://doi.org/10.1016/j.jwpe.2019.101009.
[4] S. Sharma, A. Bhattacharya, Drinking water contamination and treatment techniques, Appl. Water Sci. 7 (2017) 1043–1067, https://doi.org/10.1007/s13201-016-0455-7.
[5] A. Gičević, L. Hindija, A. Karačić, Toxicity of azo dyes in pharmaceutical industry, IFMBE Proc 73 (2020) 581–587, https://doi.org/10.1007/978-3-030-17971-7_88.
[6] M. Hajimahmoodi, M. Afsharimanesh, G. Moghaddam, N. Sadeghi, M.R. Oveisi, B. Jannat, E. Pirhadi, F. Zamani Mazdeh, H. Kanan, Determination of eight synthetic dyes in foodstuffs by green liquid chromatography, Food Addit. Contam. Part A Chem. Anal. Control. Expo. Risk Assess. 30 (2013) 780–785, https://doi.org/10.1080/19440049.2013.774465.
[7] E. Guerra, M. Llompart, C. Garcia-Jares, Analysis of dyes in cosmetics: challenges and recent developments, Cosmetics 5 (2018) 1–15, https://doi.org/10.3390/COSMETICS5030047.
[8] C. Fleischmann, M. Lievenbrück, H. Ritter, Polymers and dyes: developments and applications, Polymers (Basel) 7 (2015) 717–746, https://doi.org/10.3390/polym7040717.
[9] L.I.A. Ali, H.K. Ismail, H.F. Alesary, H.Y. Aboul-Enein, A nanocomposite based on polyaniline, nickel and manganese oxides for dye removal from aqueous solutions, Int. J. Environ. Sci. Technol. (2020), https://doi.org/10.1007/s13762-020-02961-0.
[10] B. Lellis, C.Z. Fávaro-Polonio, J.A. Pamphile, J.C. Polonio, Effects of textile dyes on health and the environment and bioremediation potential of living organisms,

Biotechnol. Res. Innov. 3 (2019) 275–290, https://doi.org/10.1016/j.biori.2019.09.001.
[11] A. Salama, A. Mohamed, N.M. Aboamera, T.A. Osman, A. Khattab, Photocatalytic degradation of organic dyes using composite nanofibers under UV irradiation, Appl. Nanosci. 8 (2018) 155–161, https://doi.org/10.1007/s13204-018-0660-9.
[12] T.C. Prathna, S.K. Sharma, M. Kennedy, Nanoparticles in household level water treatment: an overview, Separ. Purif. Technol. 199 (2018) 260–270, https://doi.org/10.1016/j.seppur.2018.01.061.
[13] J. Brame, Q. Li, P.J.J. Alvarez, Nanotechnology-enabled water treatment and reuse: emerging opportunities and challenges for developing countries, Trends Food Sci. Technol. 22 (2011) 618–624, https://doi.org/10.1016/j.tifs.2011.01.004.
[14] L.M. Pandey, Surface engineering of nano-sorbents for the removal of heavy metals: interfacial aspects, J. Environ. Chem. Eng. 9 (2021) 104586, https://doi.org/10.1016/j.jece.2020.104586.
[15] S. Homaeigohar, The nanosized dye adsorbents for water treatment, Nanomaterials 10 (2020) 1–43, https://doi.org/10.3390/nano10020295.
[16] H. Voisin, L. Bergström, P. Liu, A.P. Mathew, Nanocellulose-based materials for water purification, Nanomaterials 7 (2017) 1–19, https://doi.org/10.3390/nano7030057.
[17] T.W.M. Amen, O. Eljamal, A.M.E. Khalil, N. Matsunaga, Wastewater degradation by iron/copper nanoparticles and the microorganism growth rate, J. Environ. Sci. (China). 74 (2018) 19–31, https://doi.org/10.1016/j.jes.2018.01.028.
[18] N. Savage, M.S. Diallo, Nanomaterials and water purification: opportunities and challenges, J. Nanoparticle Res. 7 (2005) 331–342, https://doi.org/10.1007/s11051-005-7523-5.
[19] M.B. Gawande, A. Goswami, F.X. Felpin, T. Asefa, X. Huang, R. Silva, X. Zou, R. Zboril, R.S. Varma, Cu and Cu-based nanoparticles: synthesis and applications in catalysis, Chem. Rev. 116 (2016) 3722–3811, https://doi.org/10.1021/acs.chemrev.5b00482.
[20] S.M. Ibrahim, A.A. Badawy, H.A. Essawy, Improvement of dyes removal from aqueous solution by Nanosized cobalt ferrite treated with humic acid during coprecipitation, J. Nanostruct. Chem. 9 (2019) 281–298, https://doi.org/10.1007/s40097-019-00318-9.
[21] M. Tulinski, M. Jurczyk, Nanomaterials synthesis methods, Metrol. Stand. Nanotechnol. 75–98 (2017), https://doi.org/10.1002/9783527800308.ch4.
[22] A.K. Mittal, Y. Chisti, U.C. Banerjee, Synthesis of metallic nanoparticles using plant extracts, Biotechnol. Adv. 31 (2013) 346–356, https://doi.org/10.1016/j.biotechadv.2013.01.003.
[23] S. Akbar, Handbook of 200 Medicinal Plants, 2020, https://doi.org/10.1007/978-3-030-16807-0.
[24] S. Iravani, Green synthesis of metal nanoparticles using plants, Green Chem. 13 (2011) 2638–2650, https://doi.org/10.1039/c1gc15386b.
[25] F. Parveen, B. Sannakki, M.V. Mandke, H.M. Pathan, Copper nanoparticles: synthesis methods and its light harvesting performance, Sol. Energy Mater. Sol. Cells 144 (2016) 371–382, https://doi.org/10.1016/j.solmat.2015.08.033.
[26] S. Yaseen, S. Zeebaree, A. Yaseen, S. Zeebaree, Synthesis of copper nanoparticles as oxidising catalysts for multi-component reactions for synthesis of 1 , 3 , 4-thiadiazole derivatives at ambient temperature, Sustain. Chem. Pharm. 13 (2019) 100155, https://doi.org/10.1016/j.scp.2019.100155.
[27] A. Esteban-Cubillo, C. Pecharromán, E. Aguilar, J. Santarén, J.S. Moya, Antibacterial activity of copper monodispersed nanoparticles into sepiolite, J. Mater. Sci. 41 (2006) 5208–5212, https://doi.org/10.1007/s10853-006-0432-x.
[28] S. Yaseen, S. Zeebaree, A. Yaseen, S. Zeebaree, O. Ismail, H. Zebari, Diagnosis of the multiple effect of selenium nanoparticles decorated by Asteriscus graveolens components in inhibiting HepG2 cell proliferation, Sustain. Chem. Pharm. 15 (2020) 100210, https://doi.org/10.1016/j.scp.2019.100210.
[29] A. Hatamie, B. Zargar, A. Jalali, Copper nanoparticles: a new colorimetric probe for quick, naked-eye detection of sulfide ions in water samples, Talanta 121 (2014) 234–238, https://doi.org/10.1016/j.talanta.2014.01.008.
[30] A. Dhaka, C.K. Githala, R. Trivedi, Green synthesis of copper nanoparticles using Celastrus paniculatus Willd . leaf extract and their photocatalytic and antifungal properties, Biotechnol. Rep. 27 (2020), e00518, https://doi.org/10.1016/j.btre.2020.e00518.
[31] S. Joshi, V.K. Garg, N. Kataria, K. Kadirvelu, Applications of Fe3O4@AC nanoparticles for dye removal from simulated wastewater, Chemosphere 236 (2019) 124280, https://doi.org/10.1016/j.chemosphere.2019.07.011.
[32] R.D. Kale, P.B. Kane, Colour removal using nanoparticles, Text. Cloth. Sustain. 2 (2017) 7, https://doi.org/10.1186/s40689-016-0015-4, 2–7.
[33] S. Sharma, A. Hasan, N. Kumar, L.M. Pandey, Removal of methylene blue dye from aqueous solution using immobilized Agrobacterium fabrum biomass along with iron oxide nanoparticles as biosorbent, Environ. Sci. Pollut. Res. 25 (2018) 21605–21615, https://doi.org/10.1007/s11356-018-2280-z.
[34] A. Afkhami, R. Moosavi, Adsorptive removal of Congo red, a carcinogenic textile dye, from aqueous solutions by maghemite nanoparticles, J. Hazard Mater. 174 (2010) 398–403, https://doi.org/10.1016/j.jhazmat.2009.09.066.
[35] T. Sinha, M. Ahmaruzzaman, Green synthesis of copper nanoparticles for the efficient removal (degradation) of dye from aqueous phase, Environ. Sci. Pollut. Res. 22 (2015) 20092–20100, https://doi.org/10.1007/s11356-015-5223-y.
[36] S.Y. Sharaf Zeebaree, A.Y. Sharaf Zeebaree, Synthesis of copper nanoparticles as oxidising catalysts for multi-component reactions for synthesis of 1,3,4- thiadiazole derivatives at ambient temperature, Sustain. Chem. Pharm. 13 (2019) 100155, https://doi.org/10.1016/j.scp.2019.100155.
[37] L. Azeez, A. Lateef, S.A. Adebisi, A.O. Oyedeji, Novel biosynthesized silver nanoparticles from cobweb as adsorbent for Rhodamine B: equilibrium isotherm, kinetic and thermodynamic studies, Appl. Water Sci. 8 (2018) 1–12, https://doi.org/10.1007/s13201-018-0676-z.
[38] D. Paul, A review on biological activities of common mallow (malva sylvestris l.), Innovare J. Life sci. 4 (2016) 1–5.
[39] F.A. Terninko, I. I, U.E. Onishchenko, Phenolic compounds Malva sylvestris by high performance liquid chromatography, PHARMA Innov. - J. Res. 3 (2014) 46–50.
[40] C.A.F. Martins, A.M. Weffort-Santos, J.C. Gasparetto, A.C.L.B. Trindade, M.F. Otuki, R. Pontarolo, Malva sylvestris L. extract suppresses desferrioxamine-induced PGE2 and PGD2 release in differentiated U937 cells: the development and validation of an LC-MS/MS method for prostaglandin quantification, Biomed. Chromatogr. 28 (2014) 986–993, https://doi.org/10.1002/bmc.3106.
[41] D. Benhammada, A. Trache, Green synthesis of CuO nanoparticles using Malva sylvestris leaf extract with different copper precursors and their effect on nitrocellulose thermal behavior, J. Therm. Anal. Calorim. 4 (2021) 1–13.
[42] D. Gao, J. Zhang, J. Zhu, J. Qi, Z. Zhang, W. Sui, H. Shi, D. Xue, Vacancy-mediated magnetism in pure copper oxide nanoparticles, Nanoscale Res. Lett. 5 (2010) 769–772, https://doi.org/10.1007/s11671-010-9555-8.
[43] H.H. Lin, C.Y. Wang, H.C. Shih, J.M. Chen, C. Te Hsieh, Characterizing well-ordered CuO nanofibrils synthesized through gas-solid reactions, J. Appl. Phys. 95 (2004) 5889–5895, https://doi.org/10.1063/1.1690114.
[44] O.I.H. Zebari, S.Y.S. Zeebaree, A.Y.S. Zeebaree, H.I.H. Zebari, H.R. Abbas, Antibacterial activity of copper nanoparticles fabricate via malva sylvesteris leaf extract, Kurdistan J. Appl. Res. (2019) 146–156, https://doi.org/10.24017/science.2019.
[45] R. Sankar, A. Karthik, A. Prabu, S. Karthik, K.S. Shivashangari, V. Ravikumar, Origanum vulgare mediated biosynthesis of silver nanoparticles for its antibacterial and anticancer activity, Colloids Surf. B Biointerfaces 108 (2013) 80–84, https://doi.org/10.1016/j.colsurfb.2013.02.033.
[46] M. Rafique, A.J. Shaikh, R. Rasheed, M.B. Tahir, S.S.A. Gillani, A. Usman, M. Imran, A. Zakir, Z.U.H. Khan, F. Rabbani, Aquatic biodegradation of methylene blue by copper oxide nanoparticles synthesized from Azadirachta indica leaves extract, J. Inorg. Organomet. Polym. Mater. 28 (2018) 2455–2462, https://doi.org/10.1007/s10904-018-0921-9.
[47] P. Thakur Saruchi, V. Kumar, Kinetics and thermodynamic studies for removal of methylene blue dye by biosynthesize copper oxide nanoparticles and its antibacterial activity, J. Environ. Heal. Sci. Eng. 17 (2019) 367–376, https://doi.org/10.1007/s40201-019-00354-1.
[48] M. Bordbar, Z. Sharifi-Zarchi, B. Khodadadi, Green synthesis of copper oxide nanoparticles/clinoptilolite using Rheum palmatum L. root extract: high catalytic activity for reduction of 4-nitro phenol, rhodamine B, and methylene blue, J. Sol. Gel Sci. Technol. 81 (2017) 724–733, https://doi.org/10.1007/s10971-016-4239-1.
[49] A. Kerour, S. Boudjadar, R. Bourzami, B. Allouche, Eco-friendly synthesis of cuprous oxide (Cu2O) nanoparticles and improvement of their solar photocatalytic activities, J. Solid State Chem. 263 (2018) 79–83, https://doi.org/10.1016/j.jssc.2018.04.010.
[50] S.A. Yasin, S.Y.S. Zeebaree, A.Y. Sharaf Zeebaree, O.I. Haji Zebari, I.A. Saeed, The efficient removal of methylene blue dye using CuO/PET nanocomposite in aqueous solutions, Catalysts 11 (2021) 241, https://doi.org/10.3390/catal11020241.
[51] A. Muthuvel, M. Jothibas, C. Manoharan, Synthesis of copper oxide nanoparticles by chemical and biogenic methods: photocatalytic degradation and in vitro antioxidant activity, Nanotechnol. Environ. Eng. 5 (2020) 14, https://doi.org/10.1007/s41204-020-00078-w, 2–19.
[52] A. Raizada, D. Ganguly, M. Manish Mankad, R. Hari Krishna, B.M. Nagabhushana, A highly efficient copper oxide nanopowder for adsorption of methylene blue dye from aqueous medium, J. Chem. Eng. Res. 2 (2014) 249–258. http://www.deltonbooks.com.
[53] S. Sonia, S. Poongodi, P.S. Kumar, D. Mangalaraj, N. Ponpandian, C. Viswanathan, Hydrothermal synthesis of highly stable CuO nanostructures for efficient photocatalytic degradation of organic dyes, Mater. Sci. Semicond. Process. 30 (2015) 585–591, https://doi.org/10.1016/j.mssp.2014.10.012.
[54] R. Katwal, H. Kaur, G. Sharma, M. Naushad, D. Pathania, Electrochemical synthesized copper oxide nanoparticles for enhanced photocatalytic and antimicrobial activity, J. Ind. Eng. Chem. 31 (2015) 173–184, https://doi.org/10.1016/j.jiec.2015.06.021.
[55] M.T. Yagub, T.K. Sen, S. Afroze, H.M. Ang, Dye and its removal from aqueous solution by adsorption: a review, Adv. Colloid Interface Sci. 209 (2014) 172–184, https://doi.org/10.1016/j.cis.2014.04.002.
[56] D. Pathania, S. Sharma, P. Singh, Removal of methylene blue by adsorption onto activated carbon developed from Ficus carica bast, Arab. J. Chem. 10 (2017) S1445–S1451, https://doi.org/10.1016/j.arabjc.2013.04.021.
[57] Z.U.H. Khan, H.M. Sadiq, N.S. Shah, A.U. Khan, N. Muhammad, S.U. Hassan, K. Tahir, S.Z. safi, F.U. Khan, M. Imran, N. Ahmad, F. Ullah, A. Ahmad, M. Sayed, M.S. Khalid, S.A. Qaisrani, M. Ali, A. Zakir, Greener synthesis of zinc oxide nanoparticles using Trianthema portulacastrum extract and evaluation of its photocatalytic and biological applications, J. Photochem. Photobiol. B Biol. 192 (2019) 147–157, https://doi.org/10.1016/j.jphotobiol.2019.01.013.
[58] J.M. Jabar, Y.A. Odusote, K.A. Alabi, I.B. Ahmed, Kinetics and mechanisms of Congo-red dye removal from aqueous solution using activated Moringa oleifera seed coat as adsorbent, Appl. Water Sci. 10 (2020) 1–11, https://doi.org/10.1007/s13201-020-01221-3.
[59] A.R. Bagheri, M. Ghaedi, A. Asfaram, S. Hajati, A.M. Ghaedi, A. Bazrafshan, M.R. Rahimi, Modeling and optimization of simultaneous removal of ternary dyes onto copper sulfide nanoparticles loaded on activated carbon using second-derivative spectrophotometry, J. Taiwan Inst. Chem. Eng. 65 (2016) 212–224, https://doi.org/10.1016/j.jtice.2016.05.004.